Dinuclear Au(I), Au(II) and Au(III) Complexes with $(CF_2)_n$ Chains: Insights into The Role of Aurophilic Interactions in the Au(I) Oxidation

Alejandro Portugués,[a] Delia Bautista,[b] and Juan Gil-Rubio*[a]

Abstract: New dinuclear Au(I), Au(II) and Au(III) complexes containing $(CF_2)_n$ bridging chains were obtained. Metallomacrocycles $[Au_2\{\mu\text{-}(CF_2)_4\}\{\mu\text{-diphosphine}\}]$ show an uncommon figure-eight structure, the helicity inversion barrier of which is influenced by aurophilic interactions and steric constraints imposed by the diphosphine. Halogenation of $LAu(CF_2)_4AuL$ ($L = PPh_3$, PMe_3, $(dppf)_{1/2}$, $(binap)_{1/2}$) gave $[Au(II)]_2$ species, some of which display unprecedented folded structures with Au–Au bonds. Aurophilic interactions facilitate this oxidation process by preorganizing the starting $[Au(I)]_2$ complexes and lowering its redox potential. The obtained $[Au(II)]_2$ complexes undergo thermal or photochemical elimination of R_3PAuX to give Au(III) perfluorinated auracycles. Evidence of a radical mechanism for these decomposition reactions was obtained.

Introduction

The applications of gold compounds in catalysis,[1–5] medicine,[6–9] and materials science[10–12] have triggered an spectacular development of the Organometallic and Coordination Chemistry of gold during the last two decades.[13–16] One of the most captivating features of gold is aurophilicity, defined as the tendency of closed-shell Au centers to approach at short distances. Abundant manifestations of this phenomenon have been found in the conformations and supramolecular arrays of gold compounds, mainly in crystal structures, but also in solution.[17–21] Besides, these interactions influence the catalytic[22–26] properties of gold complexes. Thus, complexes containing two Au^I centers connected by a three-atom bridging ligand show enhanced activity in gold-catalyzed coupling reactions, compared to their mononuclear congeners.[23,25,26] In these systems, the aurophilic interaction enables oxidative addition of YZ reagents to the $Au^I\cdots Au^I$ unit, to give $[Au^{II}\text{-}Au^{II}]$ intermediates,[23,26] which can rearrange to $[Au^I, Au^{III}]$ species (Scheme 1). Fast reductive elimination on the Au^{III} centers produces coupling products.[27,28]

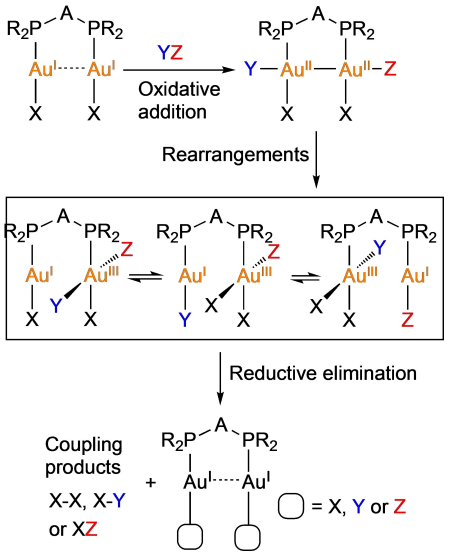

Scheme 1. Sequence of oxidative addition and reductive elimination reactions leading to coupling products in dinuclear Au complexes.

Au^{II} complexes are much less abundant than Au^I or Au^{III} ones. Most reported examples present a Au–Au covalent bond, and are obtained by oxidative addition of halogens or similar oxidants to a $Au^I\cdots Au^I$ unit containing one or two short bridging ligands.[29–31] Although Au–Au bond energies around 200 kJ/mol have been theoretically[32] and experimentally[33] determined, a very small number of stable $[Au^{II}\text{-}Au^{II}]$ complexes without supporting bridging ligands are known.[34–40]

Despite the catalytic relevance of Au^{II} complexes,[22] its reactivity has been much less explored compared to that of Au^I or Au^{III} derivatives.[29,31,37,39] Thermal rearrangement to mixed-valent $[Au^{III}, Au^I]$ species has been commonly observed,[41–44] while photochemical disproportionation[40] or reductive elimination[27,45–47] reactions have been rarely reported.

[a] A. Portugués, Dr. J. Gil-Rubio
Departamento de Química Inorgánica
Facultad de Química
Universidad de Murcia
Campus de Espinardo, 30100 Murcia (Spain)
E-mail: jgr@um.es
[b] Dr. D. Bautista
ACTI, Universidad de Murcia
Campus de Espinardo, 30100 Murcia (Spain)

Supporting information for this article is available on the WWW under https://doi.org/10.1002/chem.202103153

We have recently shown that complexes $LAu(CF_2)_4AuL$ (L = PPh_3 or PMe_3) adopt a folded structure stabilized by an aurophilic interaction (Figure 1, **A**).[21] The study of their conformational equilibria by NMR techniques provided clear evidence of the existence of aurophilic interactions in solution. Herein we report macrocyclic complexes containing two Au^I centres bridged by $(CF_2)_4$ and diphosphine ligands (Figure 1, **B**), which show an interesting dynamic behaviour. In addition, we have studied the oxidation reactions of complexes $LAu(CF_2)_4AuL$ (L = PPh_3, PMe_3, PCy_3, IPr, $(dppf)_{1/2}$, $(binap)_{1/2}$). Unprecedented [Au^{II}-Au^{II}] complexes containing a $(CF_2)_4$ chain as the only supporting bridging ligand (Figure 1, **C**), or with both $(CF_2)_4$ and diphosphine ligands (Figure 1, **D**) have been obtained. Reactivity and electrochemical studies suggest that aurophilic interactions are key for the formation of these dinuclear Au^{II} species, which undergo unprecedented thermal or photochemical rearrangements involving the cleavage and formation of Au–C bonds.

Results and Discussion

Macrocyclic Au^I complexes

The reaction of $Ph_3PAu(CF_2)_4AuPPh_3$ (**1**) with dppf or *rac*-binap gave PPh_3 and macrocyclic complexes **2** or **3**, which were isolated as soluble orange or white solids, respectively (Scheme 2). In contrast, the analogous reactions with $(CH_2)_n(PPh_2)_2$ (n = 2, 4 or 5) gave slightly soluble solids with a $[Au_2(CF_2)_4(PPh_2(CH_2)_nPPh_2)]_x$ composition, as determined by elemental analysis. The solid with n = 5 was partially soluble and showed characteristic ^{19}F NMR signals associated to the $Au(CF_2)_4Au$ chain, which were similar to those of **2**, suggesting the presence of $[Au_2\{\mu\text{-}(CF_2)_4\}\{\mu\text{-}PPh_2(CH_2)_5PPh_2\}]$ (**4**) in the soluble fraction. Oligomeric species with larger x values, could be present in the insoluble fractions.

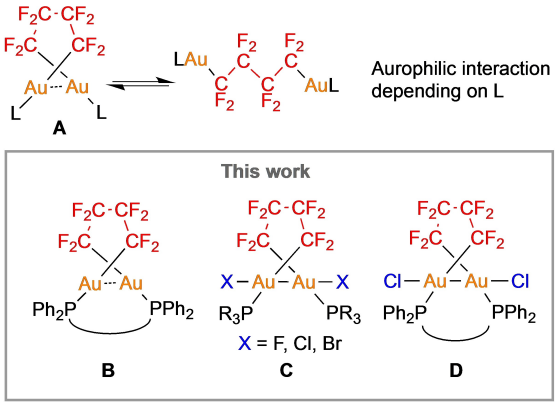

Figure 1. Previously reported dinuclear Au^I complexes (**A**). Au^I (**B**) and Au^{II} (**C**, **D**) complexes reported in this work.

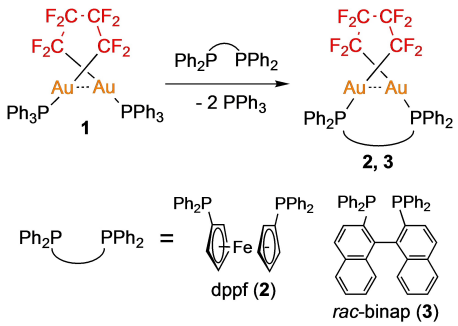

Scheme 2. Synthesis of macrocyclic dinuclear Au^I complexes.

The crystal structure of **2** shows a macrocycle formed by two Au^I centres bridged by a $(CF_2)_4$ chain and a dppf ligand (Figure 2). The ring is folded, adopting a figure-eight shape, where the Au atoms approach at short distance. Two C–H···F interactions cooperate to stabilize this conformation. Similar Au···Au and C–H···F interactions have been observed in the crystal structure of **1**.[21]

The molecule of **2** lacks any symmetry in its crystal structure, although the differences between both halves of the molecule are small. In agreement with this, at sufficiently low temperatures the ^{19}F NMR spectrum shows seven doublets corresponding to eight inequivalent ^{19}F nuclei, two of which are coincidentally isochronous. On increasing temperature these signals coalesce into four doublets, as expected for a folded ring with average C_2 symmetry (Figure 3). Further temperature increase produces the coalescence of the four doublets into two broad signals, due to fast inversion of the ring helicity in the NMR time scale. The rate constants for this inversion process were determined by line shape analysis of the ^{19}F NMR spectrum at different temperatures. An activation enthalpy of 49.1 kJ/mol was calculated by Eyring analysis,[48] which is significantly larger than the activation enthalpy determined for the helicity inversion of **1** (35.8 kJ/mol).[21] This difference is rationalized by considering that inversion of **1** can easily take place after breaking the Au···Au and C–H···F interactions and formation of an extended species, while in **2** the distance between both Au centers is constrained by the limited

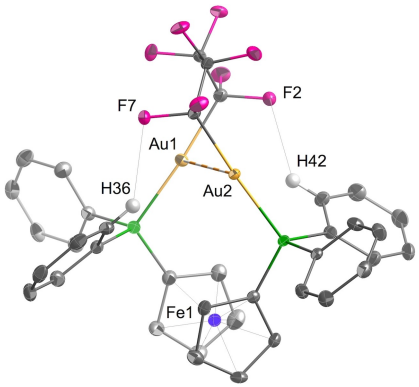

Figure 2. ORTEP diagram (thermal ellipsoids set at 50% probability) of the molecular structure of **2**. H atoms were omitted except those involved in weak interactions (Relevant distances (Å): Au1···Au2 2.9799(2), H36-F7 2.49, H42-F2 2.38).[48]

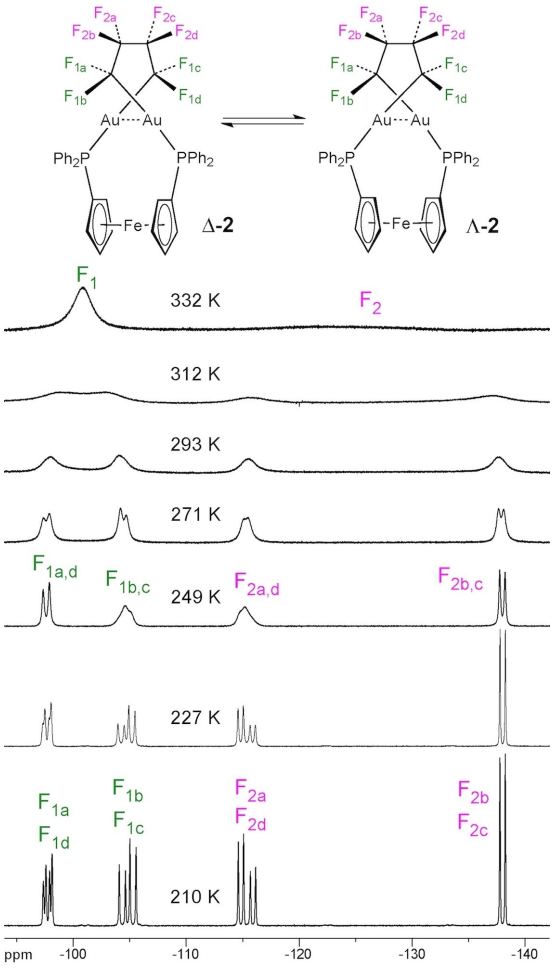

Figure 3. ^{19}F NMR spectra of **2** at selected temperatures ($CDCl_3$, 564.6 MHz). Different ^{19}F chemical environments are labelled as F_a, F_b, F_c, F_d. Interconversion between both conformers originates a/b and c/d exchange. Between 210 and 227 K the molecule adopts an unsymmetrical conformation (not shown).

conformational mobility of the macrocycle, raising the activation energy.

Similarly, the variable-temperature NMR spectra of **3** suggest that at low temperatures the macrocycle adopts an unsymmetrical conformation where all ^{19}F and ^{31}P nuclei are inequivalent (Figures S54–S56).[48] As the temperature increases ($T > 211$ K), fast conformational motion leads to an average C_2 symmetry. However, further temperature raise to 349 K did not produce coalescence of the observed signals, which is attributable to the intrinsic chirality of the binap ligand. Remarkably, only one diastereomer was observed despite racemic binap was used, which suggests that the configuration of the binaphthyl unit determines the helicity sense of the $Au(CF_2)_4Au$ chain. The ^{19}F NMR spectrum of **4** agrees with a cyclic structure of C_2 symmetry analogous to that of **2** (Figure S57).[48]

Au^{II} and Au^{III} complexes

Oxidation of **1** or $Me_3PAu(CF_2)_4AuPMe_3$ (**5**) with an equimolar amount of $PhICl_2$ gave Au^{II} complexes **6** or **7**, respectively (Scheme 3), which were isolated as yellow light-sensitive solids. Photodecomposition of **6** and **7** in solution was fast under irradiation at 402 nm, giving an almost equimolar mixture of R_3PAuCl and $[Au\{\kappa^2\text{-}(CF_2)_4\}Cl(PR_3)]$ (R = Ph (**8**), Me (**9**)) in 2–5 minutes. Traces of octafluorocyclobutane were detected by NMR spectroscopy and MS. In the absence of light, conversion of **6** into Ph_3PAuCl and **8** took more than 8 days at room temperature, or 1 h at 80 °C. Photodecomposition was also observed when solid **6** was exposed to ambient light.[49]

The crystal structure of **6** shows an almost linear Cl–Au-Au–Cl unit (Figure 4). The Au–Au distance shortens from 3.0394(3) Å in **1** to 2.5454(3) Å in **3**, a value that is comparable to those found in the two reported perfluoroalkyl Au^{II} complexes, $[Au(CF_3)_2(py)]_2$[35] and $[Au_2(CF_3)_2\{\mu\text{-}(CH_2)_2PPh_2\}]$[50] (Au–Au distances: 2.5062(9) and 2.679(1) Å, respectively). Owing to the reduction of the Au–Au distance, the P–Au-Au–P dihedral angle is larger for **6** (96.177°) than for **1** (72.299°). The looped structure is chiral and both enantiomers are present in the unit cell. Although the molecule does not present any crystallographic symmetry element, its geometry is very close to that expected for an ideal C_2 symmetry.

The ^{19}F and $^{31}P\{^1H\}$ NMR spectra of **6** and **7** are very similar and suggest that the main features of the solid-state structure of **6** are essentially maintained in solution for both complexes. Thus, the room temperature ^{19}F NMR spectra show four sharp signals corresponding to a C_2-symmetric species, indicating that the covalent Au–Au bond hampers the inversion of the loop. By

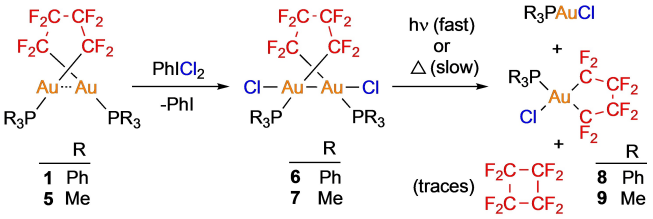

Scheme 3. Oxidation of dinuclear Au^I complexes and decomposition of the resulting Au^{II} complexes.

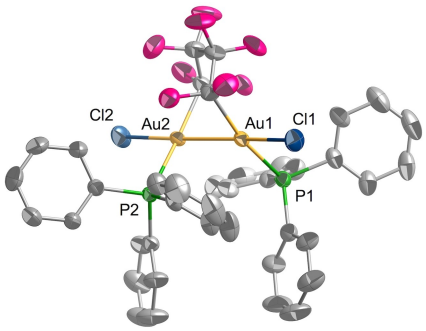

Figure 4. ORTEP diagram (thermal ellipsoids set at 50% probability, H atoms omitted) of the molecular structure of **6**.[48]

contrast, the weak non-covalent interactions that stabilize the folded conformation in **1** and **5** can be broken at relatively low temperatures.

The reactions of **1** or **5** with $PhICl_2$ in a 1:2 molar ratio gave mainly complexes **6** or **7** instead of the expected dinuclear Au^{III} species resulting from dichlorination of each gold centre. The formation of the Au^{II} complexes was fast, but subsequent reaction with $PhICl_2$ was sluggish. Indeed, at long reaction times (24 h), unreacted $PhICl_2$, **6** or **7**, and their decomposition products (**8** or **9** and LAuCl) were observed.[48]

To get a closer insight into the influence of the auxiliary ligands in the stability of the Au^{II} dinuclear complexes, we carried out the reactions of $LAu(CF_2)_4AuL$ (L = PCy_3 (**10**) or IPr (**11**)) with $PhICl_2$. We have previously observed that bulky ligands disfavour the folded conformation of these dinuclear Au^{I} complexes.[21] Thus, considering the shorter Au–Au distance in the Au^{II} complexes, we expected that an increase of the bulkiness of L should have a substantial effect in the outcome of these reactions. In line with this, no Au^{II} complexes were detected in the reactions of **10** or **11** with an equimolar amount of $PhICl_2$ (Scheme 4). In the reaction with **10**, the main products were Cy_3PAuCl and **12**, likely formed by decomposition of the unstable dinuclear Au^{II} intermediate **A**. Small amounts of Au^{III} complexes (**13** and **14**) were observed. By contrast, the reaction of **11** with $PhICl_2$ led to complexes resulting mainly from dichlorination of one (**15**) or both (**16**) metal atoms, and complex **17**. Remarkably, no $[Au\{\kappa^2\text{-}(CF_2)_4\}Cl(IPr)]$ was detected in the reaction mixture. Compound **16** was the main product in the reaction of **11** with 2 equivalents of $PhICl_2$. Small amounts of unidentified products were also formed in these reactions, accounting for less than 9% of the total integral of the ^{19}F NMR spectra of the mixtures.

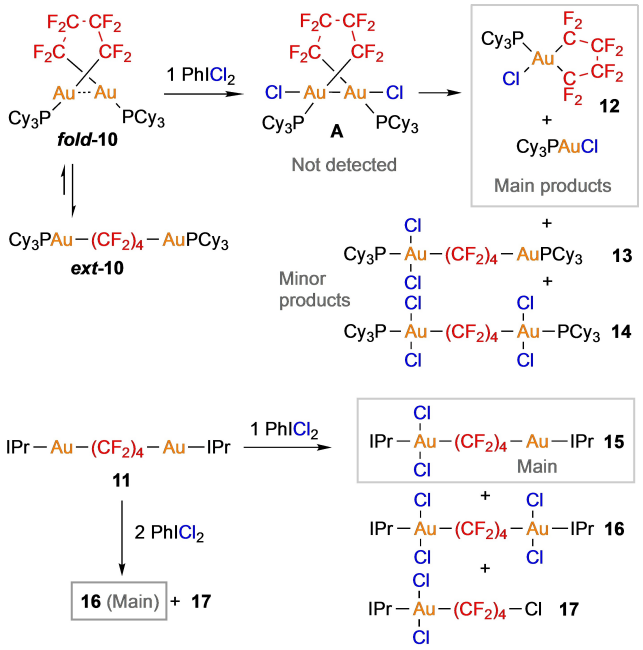

Scheme 4. Reactions of Au^{I} complexes containing bulky ligands with $PhICl_2$.

The reaction of $Ph_3PAu(CF_2)_6AuPPh_3$ (**18**) with an equimolar amount of $PhICl_2$ gave a mixture of Au^{I} and Au^{III} species resulting from partial chlorination of the metal atoms and Au–C bonds (Scheme 5). No Au^{II} complexes were detected. The ^{19}F and $^{31}P\{^1H\}$ NMR spectra showed characteristic NMR signals for the Ph_3PAuCF_2- and $Ph_3PAu(Cl)_2CF_2$- moieties, but an unambiguous identification of the components of the mixture was not possible because of extensive signal overlapping.[48] The reaction of **18** with $PhICl_2$ in a 1:2 molar ratio gave **19**, which was isolated.

Reaction of **1** with XeF_2 in CD_2Cl_2 gave the fluorocomplex **20** (Scheme 6). **20** is light sensitive and thermally unstable in solution at room temperature. Its decomposition produced an untractable mixture, where only $[Au\{\kappa^2\text{-}(CF_2)_4\}F(PPh_3)]$ (**21**) could be identified by NMR spectroscopy. Similarly, the reaction of **1** with Br_2 gave the bromocomplex **22**, which decomposed in the dark at room temperature to give $[Au\{\kappa^2\text{-}(CF_2)_4\}Br(PPh_3)]$ (**23**) and Ph_3PAuBr. Owing to their instability, **20** and **22** could not be isolated. The reaction of **1** with I_2 gave mainly Ph_3PAuI and $[Au\{\kappa^2\text{-}(CF_2)_4\}I(PPh_3)]$.[21]

Remarkably, complex **20** and $[Au_2F_2(\mu\text{-dfmt})_2]$ (dfmt = *N*,*N*′-bis(2,6-dimethylphenyl)formamidinate),[51] are the only Au^{II} fluorocomplexes reported.[52] The gold-bound fluorine atoms in **20** were evidenced in its ^{19}F NMR spectrum by a broad singlet at −186.1 ppm. The ^{19}F NMR signals of the $(CF_2)_4$ chain and the $^{31}P\{^1H\}$ NMR signals of **20** and **22** were similar to those of **6** and **7**, and agree with a similar structure of C_2 symmetry. Auracyclic complexes **21** and **23** were identified by means of their characteristic ^{19}F and $^{31}P\{^1H\}$ NMR signals, which were compared with those of samples generated by halide substitution in $[Au\{\kappa^2\text{-}(CF_2)_4\}I(PPh_3)]$.[48]

Oxidation of complexes **2** or **3** with an equimolar amount of $PhICl_2$ gave Au^{II} macrocyclic complexes **24** or **25** (Scheme 7), which were isolated as brown or yellow solids, respectively. Both are light-sensitive in solution, but in the mixtures of decomposition products only the anionic complex $[Au\{\kappa^2\text{-}(CF_2)_4\}Cl_2]^-$ could be identified by NMR spectroscopy. The oxidation of Au^{I} dinuclear macrocyclic complexes to $[Au^{II}\text{-}Au^{II}]$ complexes

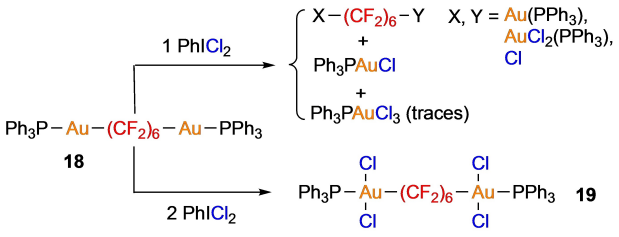

Scheme 5. Reaction of a Au^{I} complex containing a $(CF_2)_6$ chain with $PhICl_2$.

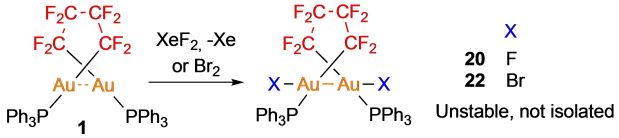

Scheme 6. In situ formation of Au^{II} fluoro- or bromo-complexes.

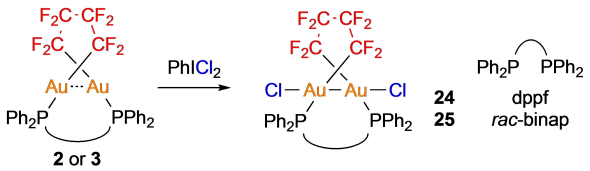

Scheme 7. Reactions of dinuclear macrocyclic complexes with $PhICl_2$.

has been previously observed in macrocyclic bis-carbene complexes.[53–55]

The crystal structure of **24** shows an almost linear Cl–Au-Au–Cl unit (Figure 5), with a Au–Au distance (2.5274(3) Å) similar to that of **6** (2.5454(3) Å). The $PAu(CF_2)_4AuP$ chain also adopts a looped conformation, although the PAuAuP dihedral angle (84.827°) is smaller than in **6** because of the conformational constraints imposed by the diphosphine ligand. Both enantiomers of **24** are present in the unit cell. The ferrocenediyl unit is not symmetrically disposed, making both halves of the molecule significantly different.

As observed for the other dinuclear Au^{II} complexes **6**, **7**, **20** and **22**, the ^{19}F NMR spectra of the macrocyclic Au^{II} complexes **24** and **25** show four sharp doublets of multiplets corresponding to two diastereotopic CF_2 units, in agreement with an average C_2 symmetry. The $\delta(^{19}F)$, and $^2J_{PF}$ values are similar to those of the other members of the series.

Cyclic voltammetry

To gain information about the influence of the neutral ligands and the length of the $(CF_2)_n$ chain on the outcome of the oxidation reactions of dinuclear Au^I complexes, we carried out cyclic voltammetry measurements on complexes $LAu(CF_2)_4AuL$ (L = PPh_3 (**1**), PCy_3 (**10**), IPr (**11**)) and $LAu(CF_2)_6AuL$ (L = PPh_3 (**18**), Cy_3P). Mononuclear complexes $LAu(n\text{-}C_4F_9)$ (L = PPh_3, IPr)[56] were also studied for the purpose of comparison. The potential was scanned in the oxidative direction until solvent oxidation became dominant. Then, the scan direction was reversed toward negative values.

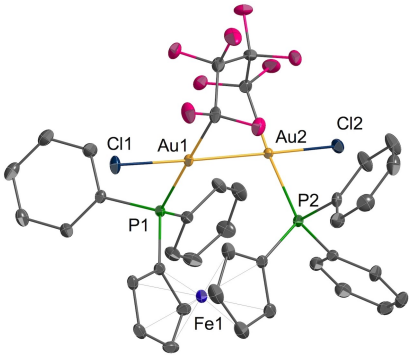

Figure 5. ORTEP diagram (thermal ellipsoids set at 50% probability, H atoms omitted) of the molecular structure of **24**.[48]

Complex **1** gave a well-defined anodic wave at a peak potential of 1.13 V, followed by another ill-defined wave around 1.5 V (Figure 6 and Table 1). Further anodic processes around 2 V were overlapped with the solvent oxidation wave. No corresponding reduction events were observed when the scan direction was reversed, which suggests that the observed oxidations are irreversible processes. The cyclic voltammogram of **10** was similar, showing a well-defined oxidation wave at 1.33 V, followed another one at ca. 2.4 V. In contrast, **11** showed a weak shoulder around 1.6 V, followed by a well-defined peak at 2.12 V. The oxidation of the other studied complexes occurred at significantly higher potential values. For instance, the first-oxidation waves of $LAu(n\text{-}C_4F_9)$ (L = Ph_3P, IPr) were observed at 2.09 and 2 V, respectively, while dinuclear complexes $LAu(CF_2)_6AuL$ (L = PPh_3 (**18**) or Cy_3P) did not show any detectable oxidation event at potentials lower than 2 V. In summary, complexes **1** and **10** show significant oxidation events at potentials lower than those of dinuclear complexes with longer $(CF_2)_n$ chains or bulkier L ligands, whose oxidation potentials are similar to those of mononuclear complexes $LAu(n\text{-}C_4F_9)$ (L = PPh_3, IPr).

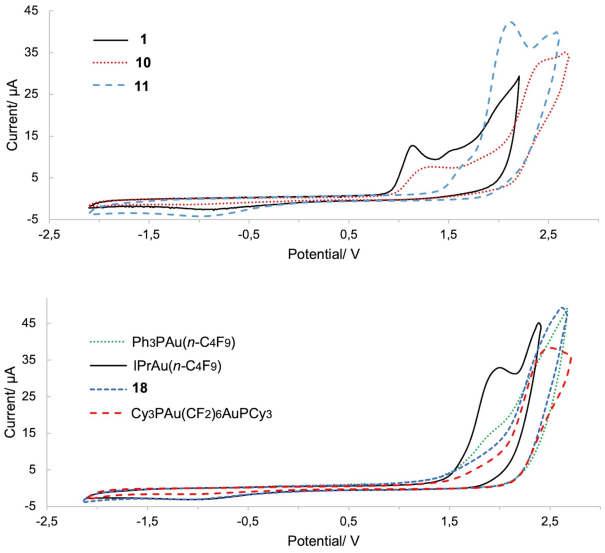

Figure 6. Cyclic voltammograms of: (top) $(CF_2)_4$-bridged; (bottom) $(CF_2)_6$-bridged and mononuclear Au^I complexes. Recorded in 0.001 M CH_2Cl_2 solutions, with 0.1 M NBu_4PF_6 as electrolyte and a 0.1 V/s scan rate.

Table 1. Electrochemical data.

Complex	E_p [V][a]
$Ph_3PAu(CF_2)_4AuPPh_3$ (**1**)	1.13, 1.5
$Cy_3PAu(CF_2)_4AuPCy_3$ (**10**)	1.33, ca. 2.4
$IPrAu(CF_2)_4AuIPr$ (**11**)	ca. 1.6[b], 2.12
$Ph_3PAu(CF_2)_6AuPPh_3$ (**18**)	>2.0
$Cy_3PAu(CF_2)_6AuPCy_3$	2.5
$Ph_3PAu(n\text{-}C_4F_9)$	2.09[c]
$IPrAu(n\text{-}C_4F_9)$	2.00

[a] Vs $FeCp_2^+/FeCp_2$. [b] Weak shoulder. [c] The observed shoulder appeared as a peak after subtraction of a blank voltammogram (see Figure S61).

Complexes **1** and **10** share in common their ability to adopt a folded structure stabilized by an aurophilic interaction. Thus, at room temperature **1** is mainly in the folded conformation and **10** is mainly in the extended one, although a significant amount of ***fold*-10** (23%) in exchange with ***ext*-10** was observed at low temperature (Scheme 4).[21] In contrast, **11**, **18** and $Cy_3PAu(CF_2)_6AuPCy_3$ display extended conformations in their crystal structures and their NMR spectra do not show any evidence of stable folded conformers.[21] This suggests that short Au···Au contacts could be responsible for the observed decrease in the first-oxidation potentials of **1** and **10**.

Cyclic voltammetry studies in dinuclear Au^{I} complexes (μ-$XZ_2)Au_2Cl_2$ (X = CH_2, Z = PPh_2 or 3-mesitylimidazol-1-yl-2-ylidene;[23] X = N(*i*-Pr), Z = PPh_2[26]) have shown that the oxidation potentials of these complexes were 0.12-0.32 V lower than those of structurally similar mononuclear complexes. We have observed larger differences ($\Delta E \geq 0.9$ V) between **1** and $Ph_3PAu(n\text{-}C_4F_9)$ or $Ph_3PAu(CF_2)_6AuPPh_3$, or between **10** and $Cy_3PAu(CF_2)_6AuPCy_3$. These larger differences can be attributed to a destabilization of the HOMO of the folded conformers of **1** and **10** induced by the stronger aurophilic interactions.

Mechanistic considerations

Reaction pathways leading to the observed products are outlined in Scheme 8. Chlorination of the initial dinuclear Au^{I} complex would give a dinuclear Au^{II} complex (**B**) or a mixed-valent complex (**C**). Products of the type **B** were formed when the starting complex has a $(CF_2)_4$ chain and PPh_3, PMe_3, dppf or binap as neutral ligands. In contrast, complexes of the type **C** are formed if the gold centers are bridged by a longer chain, as in **18**, or if L is a bulky ligand, as in **11**. In these cases, **C** undergoes further chlorination to form dinuclear Au^{III} complexes (**D**). Reductive elimination with formation of a C–Cl bond from the Au^{III} centers would afford LAuCl and products of the type **E**. Complexes **B** evolve by photo- or thermally activated elimination of LAuCl to give **F**. Remarkably, disproportionation of **B** to give **C** was not observed,[42] whereas oxidation of complexes **B** with $PhICl_2$ was sluggish (observed for **6** and **7**).

An interesting case is the reaction of **10** with one equivalent of $PhICl_2$, which gives mainly Cy_3PAuCl and [Au{κ^2-$(CF_2)_4$}Cl(PCy_3)] (**12**). Since complexes of the types LAuCl and **F** are typically formed by decomposition of dinuclear Au^{II} complexes, the main reaction product should be a complex of the type **B**. The steric repulsions between the bulky PCy_3 ligands could render this intermediate unstable, provoking fast decomposition to Cy_3PAuCl and **12**. Small amounts of products of the type **C** or **D**, resulting from dichlorination of the Au centres, were observed in this reaction.

We hypothesize that the close approach of the Au centers in the starting dinuclear Au^{I} complexes is beneficial for the formation of complexes **B** in two ways. Firstly, it lowers the redox potential at which the first oxidation occurs, as observed for **1** and **10**. Secondly, it would stabilize the initially formed [Au^{II}, Au^{I}] species, which could undergo a further one-electron oxidation to give [Au^{II}-Au^{II}] complexes (**B**). If the separation of the Au atoms is large, the [Au^{II}, Au^{I}] intermediates would be oxidized to [Au^{III}, Au^{I}] species and then to [Au^{III}, Au^{III}] complexes.

The fast photodecomposition of complexes **B** and the detection of octafluorocyclobutane are indicative of a radical reaction. In agreement with this, the yield of the decomposition of **6** was reduced in the presence of TEMPO from 100% to 77% (photochemical) or 65% (thermal), and the radical-trapping diadduct $(TEMPO)_2(\mu\text{-}C_4F_8)$[21] was observed (6% in the photodecomposition, traces in the thermal decomposition). This suggests that homolysis of the Au-CF_2 bonds takes place during the decomposition of **6**. To test if the observed octafluorocyclobutane could be formed by decomposition of a complex of the type **F**, [Au{κ^2-$(CF_2)_4$}I(PPh_3)] was heated (100 °C, toluene) or irradiated (402 or 310 nm, CD_2Cl_2). However, no octafluorocyclobutane was detected in these experiments.

Theoretical studies on binuclear Au^{II} complexes suggest that the LUMO of these complexes has Au–Au and Au-halogen antibonding character.[30,45,57,58] In line with this, photoexcitation of **6** could lead to weakening of the Au–Au bond facilitating its homolysis to give radical intermediates (Scheme 9), which would eliminate a molecule of Ph_3PAuCl. The resulting diradical (**G**), could undergo an intramolecular coupling, to give auracycle **8**. This would constitute the main decomposition pathway, but **G** could also give Ph_3PAuCl and C_4F_8. Diadduct $(TEMPO)_2(\mu\text{-}(CF_2)_4)$ would be produced in the presence of TEMPO.

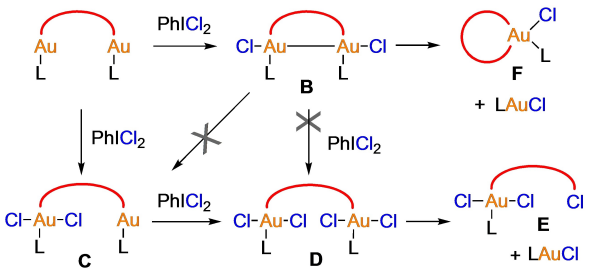

Scheme 8. Reactions leading to Au^{II}, Au^{III} and mixed-valent complexes.

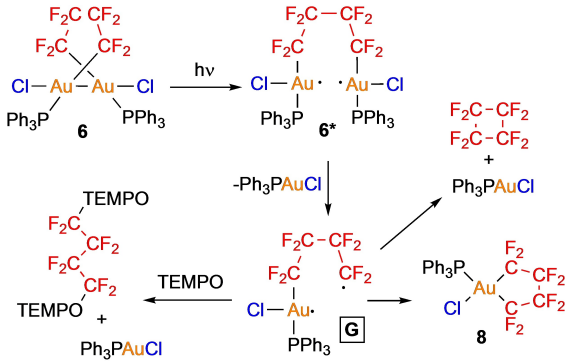

Scheme 9. Proposed decomposition mechanism for **6**.

Conclusions

We have reported the first macrocyclic complexes containing two Au^{I} centers linked by a perfluorocarbon chain, which adopt a rare figure-eight conformation. The higher energetic barrier for exchange between both enantiomeric conformers of $[Au_2\{\mu\text{-}(CF_2)_4\}(\mu\text{-diphosphine})]$ (diphosphine = dppf (**2**), binap (**3**)) respect to the acyclic analogues $R_3PAu(CF_2)_4AuPR_3$ (R = Ph (**1**) or Me (**5**)) is originated by conformational constraints imposed by the presence of the diphosphine ligands.

Complexes **1**, **2**, **3** or **5** react with halogenating agents to give dinuclear Au^{II} complexes which present unprecedented structures. In the acyclic complexes **6** and **7**, the bridging $(CF_2)_4$ chain allows the approach of both Au centres, but does not impede their separation at relatively long distances. Therefore, they constitute a new type of Au^{II} complexes having *semi-supported* Au^{II}-Au^{II} bonds.

CV studies suggest a marked lowering of the oxidation potential of the dinuclear [Au^{I}, Au^{I}] complexes induced by the presence of aurophilic interactions. This effect, together with the presence of a $(CF_2)_4$ linker between the Au^{I} centres and the low steric hindrance of the neutral ligands, is beneficial for the formation and stability of the [Au^{II}-Au^{II}] complexes. In contrast, the presence of a longer $(CF_2)_6$ linker or bulky neutral ligands in the starting [Au^{I}, Au^{I}] complexes induce the formation of [Au^{III}, Au^{I}] and [Au^{III}, Au^{III}] complexes.

Thermal or photochemical decomposition of complexes $[(AuX)_2\{\mu\text{-}(CF_2)_4\}(PR_3)_2]$ gives rise to elimination of R_3PAuX and formation of Au^{III} complexes which are new members of a rare family of perfluorinated auracycles. Evidence of a radical mechanism for these decomposition reactions has been obtained.

Acknowledgements

Financial support from Spanish Ministry of Science and Innovation/FEDER (Grant PGC2018-100719-B-100) and Séneca Foundation of the Region of Murcia (*Ayudas a Grupos de Excelencia*, grant 19890/GERM/15) is gratefully acknowledged.

Conflict of Interest

The authors declare no conflict of interest.

Keywords: aurophilicity · fluorinated ligands · gold · metallacycles · metal-metal interactions

[1] Y. Li, W. Li, J. Zhang, *Chem. Eur. J.* **2017**, *23*, 467–512.
[2] A. Corma, A. Leyva-Pérez, M. J. Sabater, *Chem. Rev.* **2011**, *111*, 1657–1712.
[3] A. S. K. Hashmi, *Chem. Rev.* **2007**, *107*, 3180–3211.
[4] Z. Li, C. Brouwer, C. He, *Chem. Rev.* **2008**, *108*, 3239–3265.
[5] A. Nijamudheen, A. Datta, *Chem. Eur. J.* **2020**, *26*, 1442–1487.
[6] T. Zou, C. T. Lum, C.-N. Lok, J.-J. Zhang, C.-M. Che, *Chem. Soc. Rev.* **2015**, *44*, 8786–8801.
[7] B. Bertrand, A. Casini, *Dalton Trans.* **2014**, *43*, 4209–4219.
[8] B. Bertrand, M. R. M. Williams, M. Bochmann, *Chem. Eur. J.* **2018**, *24*, 11840–11851.
[9] M. Mora, M. C. Gimeno, R. Visbal, *Chem. Soc. Rev.* **2019**, *48*, 447–462.
[10] V. W.-W. Yam, V. K.-M. Au, S. Y.-L. Leung, *Chem. Rev.* **2015**, *115*, 7589–7728.
[11] M.-C. Tang, M.-Y. Chan, V. W.-W. Yam, *Chem. Rev.* **2021**, *121*, 7249–7279.
[12] J. M. López-de-Luzuriaga, M. Monge, M. E. Olmos, *Dalton Trans.* **2017**, *46*, 2046–2067.
[13] R. P. Herrera, M. C. Gimeno, *Chem. Rev.* **2021**, *121*, 8311–8363.
[14] H. G. Raubenheimer, H. Schmidbaur, *J. Chem. Educ.* **2014**, *91*, 2024–2036.
[15] M. Joost, A. Amgoune, D. Bourissou, *Angew. Chem. Int. Ed.* **2015**, *54*, 15022–15045; *Angew. Chem.* **2015**, *127*, 15234–15258.
[16] L. Rocchigiani, M. Bochmann, *Chem. Rev.* **2021**, *121*, 8364–8451.
[17] H. Schmidbaur, A. Schier, *Chem. Soc. Rev.* **2012**, *41*, 370–412.
[18] H. Schmidbaur, A. Schier, *Chem. Soc. Rev.* **2008**, *37*, 1931–1951.
[19] N. Mirzadeh, S. H. Privér, A. J. Blake, H. Schmidbaur, S. K. Bhargava, *Chem. Rev.* **2020**, *120*, 7551–7591.
[20] T. P. Seifert, V. R. Naina, T. J. Feuerstein, N. D. Knöfel, P. W. Roesky, *Nanoscale* **2020**, *12*, 20065–20088.
[21] A. Portugués, L. González, D. Bautista, J. Gil-Rubio, *Angew. Chem. Int. Ed.* **2020**, *59*, 15220–15225; *Angew. Chem.* **2020**, *132*, 15332–15337.
[22] W. Wang, C.-L. Ji, K. Liu, C.-G. Zhao, W. Li, J. Xie, *Chem. Soc. Rev.* **2021**, *50*, 1874–1912.
[23] E. Tkatchouk, N. P. Mankad, D. Benitez, W. A. Goddard, F. D. Toste, *J. Am. Chem. Soc.* **2011**, *133*, 14293–14300.
[24] W. E. Brenzovich Jr., D. Benitez, A. D. Lackner, H. P. Shunatona, E. Tkatchouk, W. A. Goddard III, F. D. Toste, *Angew. Chem. Int. Ed.* **2010**, *49*, 5519–5522; *Angew. Chem.* **2010**, *122*, 5651–5654.
[25] M. D. Levin, F. D. Toste, *Angew. Chem. Int. Ed.* **2014**, *53*, 6211–6215; *Angew. Chem.* **2014**, *126*, 6325–6329.
[26] K. Liu, N. Li, Y. Ning, C. Zhu, J. Xie, *Chem* **2019**, *5*, 2718–2730.
[27] W. J. Wolf, M. S. Winslow, F. D. Toste, *Nat. Chem.* **2014**, *6*, 159–164.
[28] M. A. Bennett, D. C. R. Hockless, A. D. Rae, L. L. Welling, A. C. Willis, *Organometallics* **2001**, *20*, 79–87.
[29] A. Laguna, M. Laguna, *Coord. Chem. Rev.* **1999**, *193–195*, 837–856.
[30] A. A. Mohamed, H. E. Abdou, J. P. Fackler, *Coord. Chem. Rev.* **2010**, *254*, 1253–1259.
[31] N. Mirzadeh, M. A. Bennett, S. K. Bhargava, *Coord. Chem. Rev.* **2013**, *257*, 2250–2273.
[32] X.-G. Xiong, P. Pyykkö, *Chem. Commun.* **2013**, *49*, 2103–2105.
[33] T. Dann, D.-A. Roşca, J. A. Wright, G. G. Wildgoose, M. Bochmann, *Chem. Commun.* **2013**, *49*, 10169–10171.
[34] J. Coetzee, W. F. Gabrielli, K. Coetzee, O. Schuster, S. D. Nogai, S. Cronje, H. G. Raubenheimer, *Angew. Chem. Int. Ed.* **2007**, *46*, 2497–2500; *Angew. Chem.* **2007**, *119*, 2549–2552.
[35] D. Zopes, C. Hegemann, W. Tyrra, S. Mathur, *Chem. Commun.* **2012**, *48*, 8805–8807.
[36] S. A. Yurin, D. A. Lemenovskii, K. I. Grandberg, I. G. Il'ina, L. G. Kuz'mina, *Russ. Chem. Bull.* **2003**, *52*, 2752–2753.
[37] V. W.-W. Yam, S. W.-K. Choi, K.-K. Cheung, *Chem. Commun.* **1996**, 1173–1174.
[38] V. W.-W. Yam, C.-K. Li, C.-L. Chan, K.-K. Cheung, *Inorg. Chem.* **2001**, *40*, 7054–7058.
[39] D.-A. Roşca, D. A. Smith, D. L. Hughes, M. Bochmann, *Angew. Chem. Int. Ed.* **2012**, *51*, 10643–10646; *Angew. Chem.* **2012**, *124*, 10795–10798.
[40] D.-A. Roşca, M. Bochmann, *Organometallics* **2016**, *35*, 27–31.
[41] M. Bardaji, M. C. Gimeno, P. G. Jones, A. Laguna, M. Laguna, *Organometallics* **1994**, *13*, 3415–3419.
[42] R. Usón, A. Laguna, M. Laguna, M. N. Fraile, P. G. Jones, G. M. Sheldrick, *J. Chem. Soc. Dalton Trans.* **1986**, 291–296.
[43] N. Meyer, C. W. Lehmann, T. K.-M. Lee, J. Rust, V. W.-W. Yam, F. Mohr, *Organometallics* **2009**, *28*, 2931–2934.
[44] M. A. Bennett, S. K. Bhargava, N. Mirzadeh, S. H. Privér, J. Wagler, A. C. Willis, *Dalton Trans.* **2009**, 7537–7551.
[45] J. D. Basil, H. H. Murray, J. P. Fackler, J. Tocher, A. M. Mazany, B. Trzcinska-Bancroft, H. Knachel, D. Dudis, T. J. Delord, D. Marler, *J. Am. Chem. Soc.* **1985**, *107*, 6908–6915.
[46] M. A. Bennett, S. K. Bhargava, D. C. R. Hockless, L. L. Welling, A. C. Willis, *J. Am. Chem. Soc.* **1996**, *118*, 10469–10478.
[47] Y. Tsuchido, R. Abe, T. Ide, K. Osakada, *Angew. Chem. Int. Ed.* **2020**, *59*, 22928–22932; *Angew. Chem.* **2020**, *132*, 23128–23132.
[48] Supporting Information contains: Synthetic procedures, characterization data, NMR and mass spectra, dynamic NMR and reaction monitoring studies, crystallographic data and additional CV data. Deposition

Numbers 2088734 (for **2**), 2088732 (for **6**), and 2088733 (for **24**) contains the supplementary crystallographic data for this paper. These data are provided free of charge by the joint Cambridge Crystallographic Data Centre and Fachinformationszentrum Karlsruhe Access Structures service.

[49] Small amounts of the salt $[Au(PPh_3)_2]^+[Au\{\kappa^2\text{-}(CF_2)_4\}Cl_2]^-$ arising from ligand scrambling between **8** and Ph_3PAuCl were detected in the decomposition mixtures (see Supporting Information).

[50] H. H. Murray, J. P. Fackler, L. C. Porter, D. A. Briggs, M. A. Guerra, R. J. Lagow, *Inorg. Chem.* **1987**, *26*, 357–363.

[51] D. Y. Melgarejo, G. M. Chiarella, J. P. Fackler, L. M. Perez, A. Rodrigue-Witchel, C. Reber, *Inorg. Chem.* **2011**, *50*, 4238–4240.

[52] AuF_2 has been detected in matrix isolation experiments. See: X. Wang, L. Andrews, K. Willmann, F. Brosi, S. Riedel, *Angew. Chem. Int. Ed.* **2012**, *51*, 10628–10632; *Angew. Chem.* **2012**, *124*, 10780–10784.

[53] A. H. Mageed, B. W. Skelton, A. N. Sobolev, M. V. Baker, *Eur. J. Inorg. Chem.* **2018**, *2018*, 109–120.

[54] M. Baron, C. Tubaro, M. Basato, M. M. Natile, C. Graiff, *J. Organomet. Chem.* **2013**, *723*, 108–114.

[55] C. Tubaro, M. Baron, M. Costante, M. Basato, A. Biffis, A. Gennaro, A. A. Isse, C. Graiff, G. Accorsi, *Dalton Trans.* **2013**, *42*, 10952–10963.

[56] A. Portugués, I. López-García, J. Jiménez-Bernad, D. Bautista, J. Gil-Rubio, *Chem. Eur. J.* **2019**, *25*, 15535–15547.

[57] A. A. Mohamed, A. P. Mayer, H. E. Abdou, M. D. Irwin, L. M. Pérez, J. P. Fackler, *Inorg. Chem.* **2007**, *46*, 11165–11172.

[58] Q.-J. Pan, X. Zhou, H.-G. Fu, H.-X. Zhang, *Organometallics* **2008**, *27*, 2474–2482.

Manuscript received: August 31, 2021
Accepted manuscript online: September 7, 2021
Version of record online: September 29, 2021

